From charged-particle multiplicities to the top quark

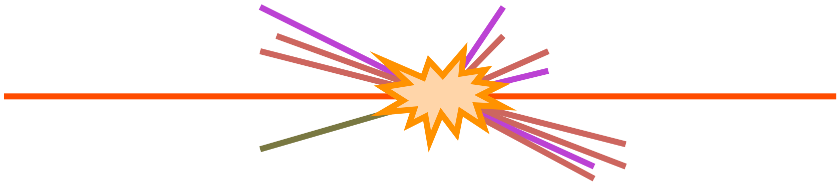

W. H. Bell

Université de Genève

Overview

- Introduction
- Charged-particle multiplicities
- Inclusive W cross-section
- W + jets cross-section
- Top cross-section
- Conclusions
- Analyses for 2011

ppbar and *pp* cross-section

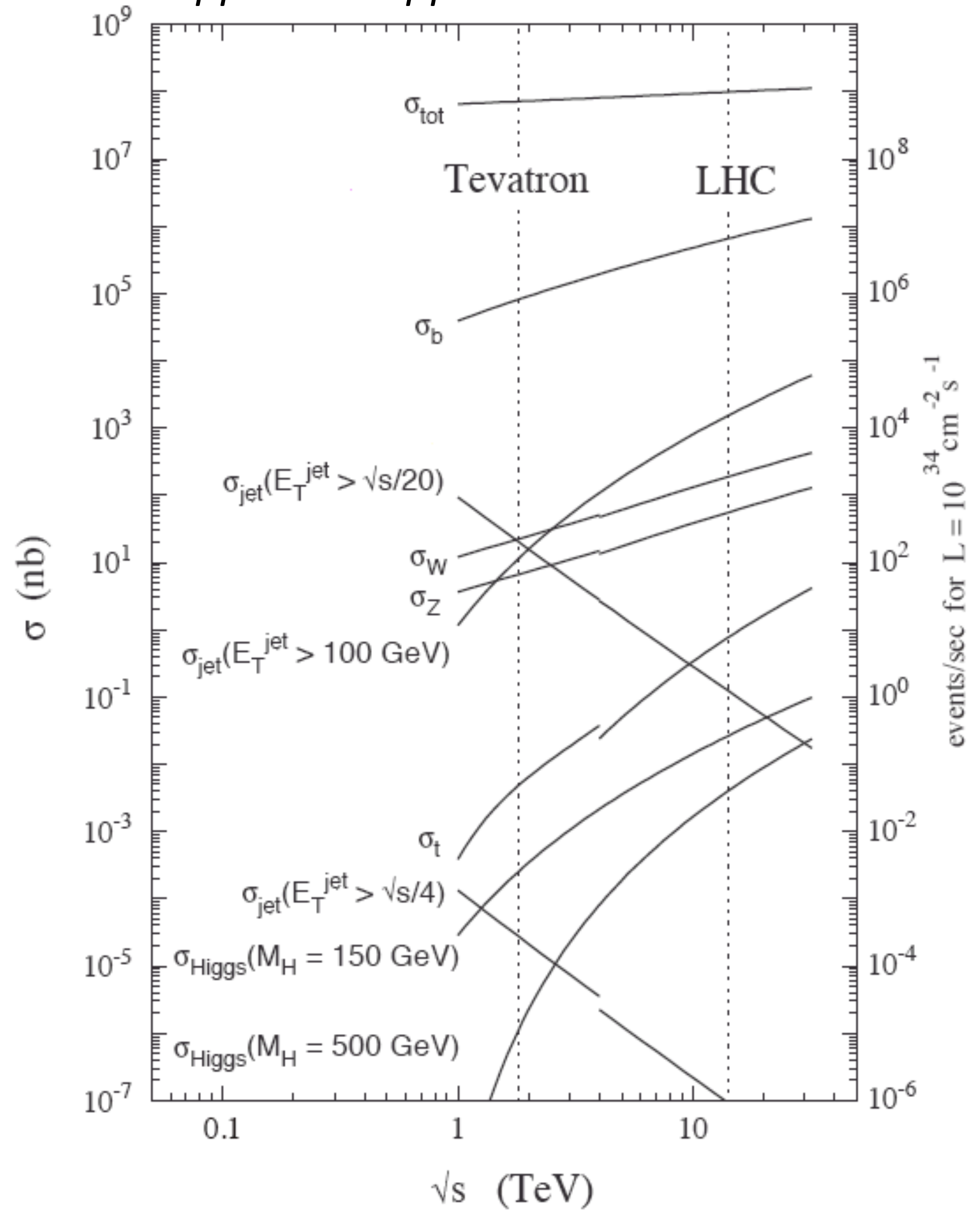

Objectives

- The LHC is a discovery machine
- Study standard model properties
- Search for the Higgs boson.
- Look for sources of new physics.

Proton-proton collision

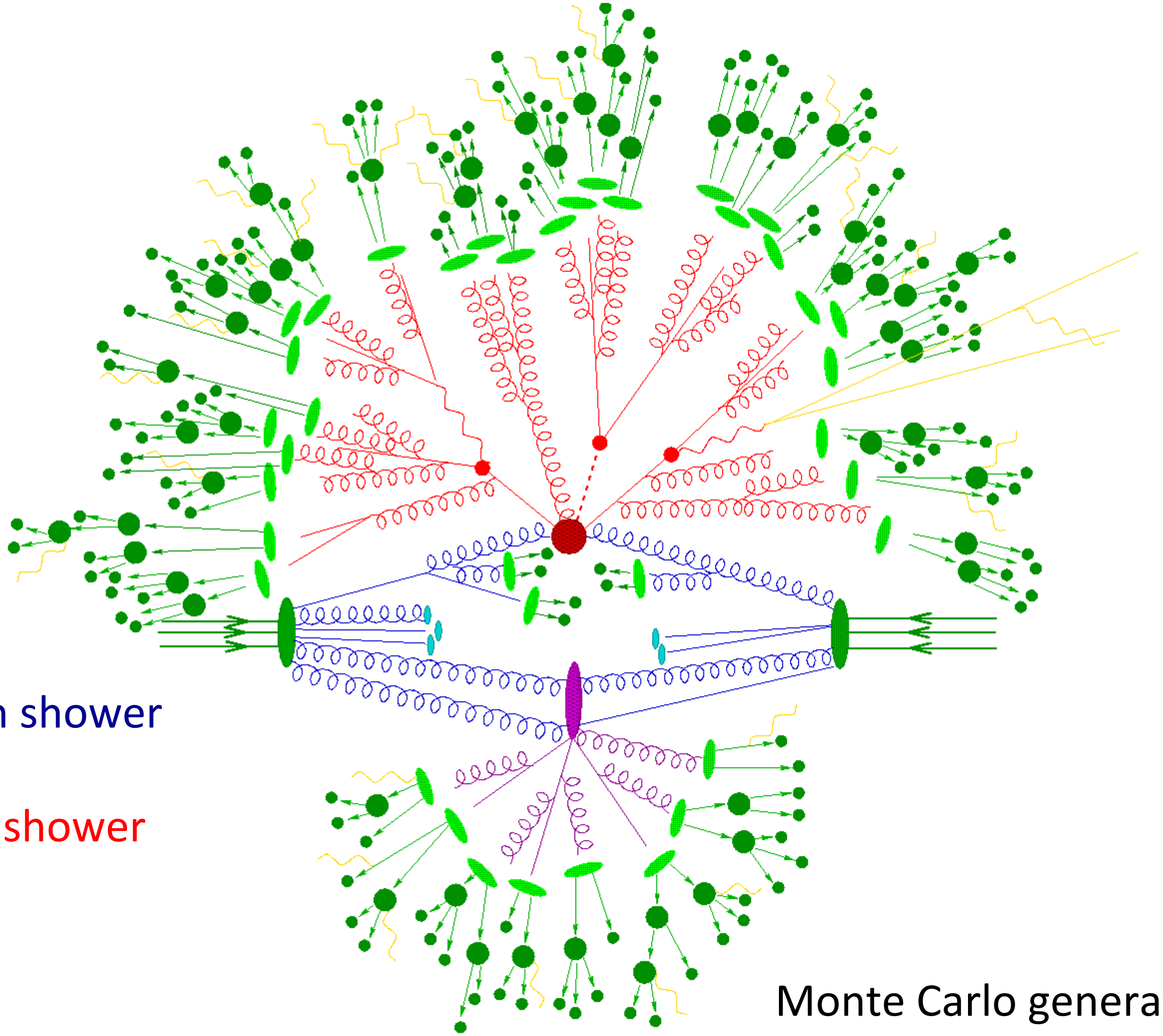

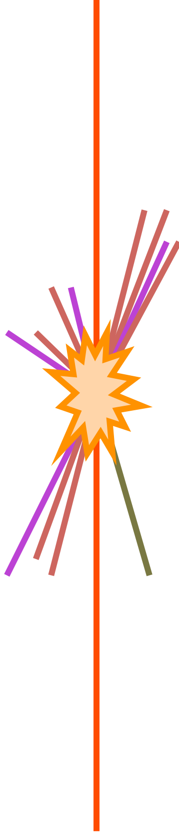

Initial state parton shower
Signal process
Final state parton shower
Fragmentation
Hadron decays
Beam remnants
Underlying event

Monte Carlo generator representation
Sherpa

The ATLAS detector

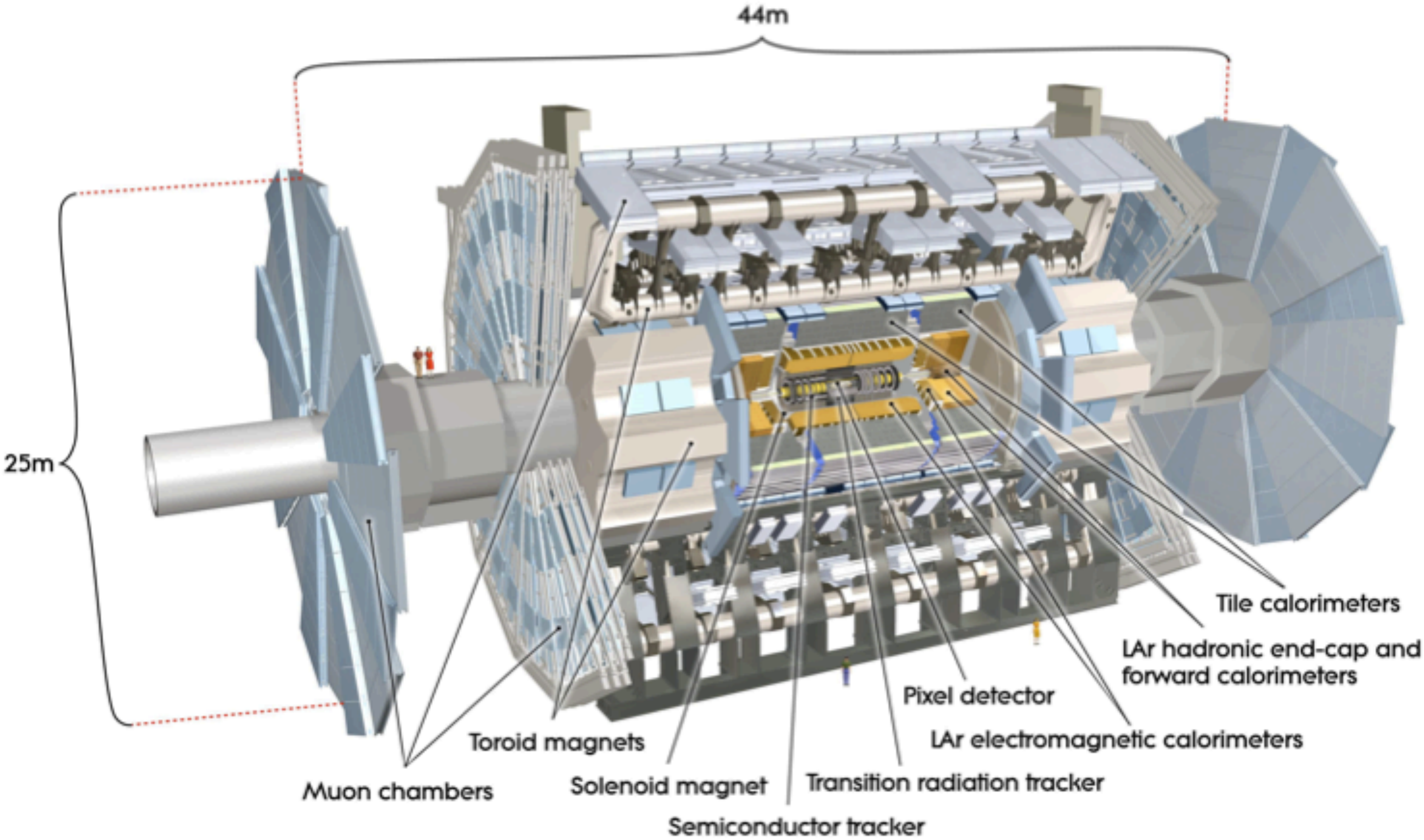

Charged-particle multiplicity distributions

- Basic underlying physics of *pp* interactions.
- MC attempt to describe low-p_T processes using 2-to-2 scatters and phenomenological models.
  - Multiple-parton scattering
  - Partonic matter distributions
  - Scattering between unresolved protons
  - Colour reconnection.
- Phenomenological models tuned using measurements.
  - Measurements needed to constrain behaviour at different centre-of-mass energies.

Making a measurement

- Select inelastic *pp* interactions using minimal bias.
  - Trigger scintillators with a large coverage overlapping with track-reconstruction volume.
  - The tracking detector itself.
  - Beam bunch requirement.
- Reconstruct charged particles using silicon or gas tracking detectors.
  - Magnetic field surrounding tracking volume needed for momentum measurements.
- Reconstruct the primary vertex or use the beam position to select primary tracks.
- Correct for event and track selection and provide a particle level result.

Experimental issues

- Additional *pp* interactions.
- Multiple scattering within tracking detector.
- Nuclear interactions, which result in badly measured tracks.
- p_T resolution as p_T becomes large.

Types of measurement

- No corrections
  - Easy to produce this result, hard for someone else outside the experiment to understand.
- Non-single-diffractive
  - Removal of single-diffractive events within acceptance.
  - Addition of double-diffractive and non-diffractive events with $n_{ch} = 0$ using MC generator.
- Fully corrected within kinematic range.
  - Data used for trigger and vertex corrections.
  - Only events with n_{ch} >= 1 included in distributions.

Correction factors

- Trigger selection is sensitive to physics processes.
  - Trigger correction with MC model folds in physics assumptions from MC into data distribution.
- Extrapolation back to $p_T = 0$.
  - Fold in model based assumptions about distribution.
- Correction of tracking acceptance using MC.
  - Folds in n_{ch} distribution from MC for low multiplicity bins.
- Need to avoid sources of model dependence and present results within acceptance.

n_{ch}=0 and diffraction

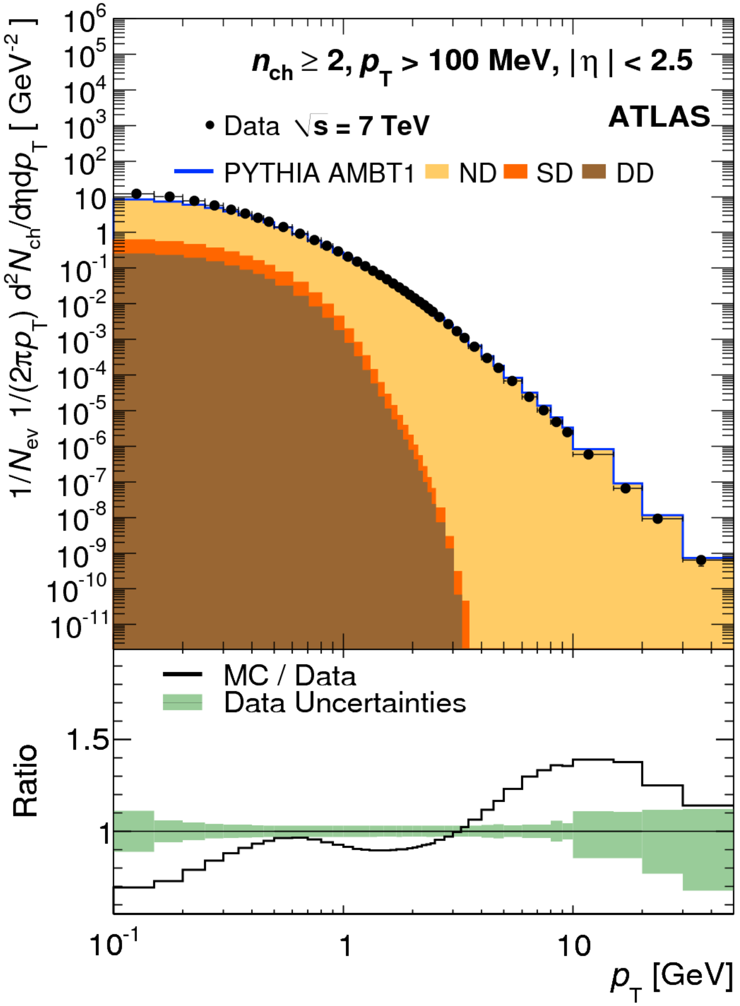

Adding in n_{ch}=0 events effects normalisation of distribution.

Removing single diffractive diffractive component implies p_T spectrum of generator removed from measured distribution.

Corrections typically made using PYTHIA 6.4.21 i.e. poor diffractive model.

These corrections are not made on the ATLAS data and this Figure is used for illustrative purposes only.

Distributions

$$\frac{1}{N_{ev}} \cdot \frac{dN_{ch}}{d\eta}$$

$$\frac{1}{N_{ev}} \cdot \frac{1}{2\pi p_T} \cdot \frac{d^2 N_{ch}}{d\eta dp_T}$$

$$\frac{1}{N_{ev}} \cdot \frac{dN_{ev}}{dn_{ch}}$$

$\langle p_T \rangle$ vs. n_{Ch}

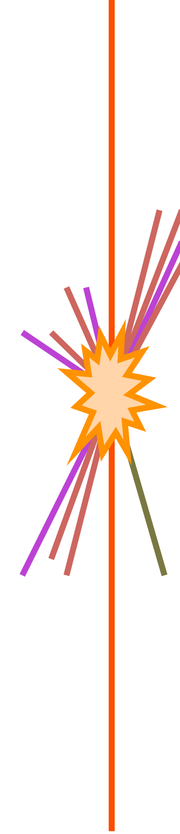

N_{ev}

N_{ch}

(1) Events with $n_{ch} \geq 1$ ($|\eta|<2.5$ & $p_T > 500\text{MeV}$)

(2) Events with $n_{ch} \geq 2$ ($|\eta|<2.5$ & $p_T > 100\text{MeV}$)

Discussion will follow (2) and √s = 7TeV measurements

Charged-particle multiplicities: summary

- Measure charged particle multiplicity distributions from inelastic events within |η|<2.5 & p_T > 100MeV
  - Require $n_{ch} \geq 2$ (|η|<2.5 & p_T > 100MeV)
    - Removes model dependence from trigger and vertex corrections.
  - No removal of single-diffractive-component.
  - No removal of Dalitz decays.
  - No extrapolation to $p_T = 0$ or correction for acceptance using models.
- Correct reconstructed-track distributions back to particle level for all detector effects.
  - Measure trigger and vertex corrections from data.

$dN_{ch}/d\eta$ $\quad$ $1/(2\pi p_T)\, d^2N_{ch}/d\eta dp_T$

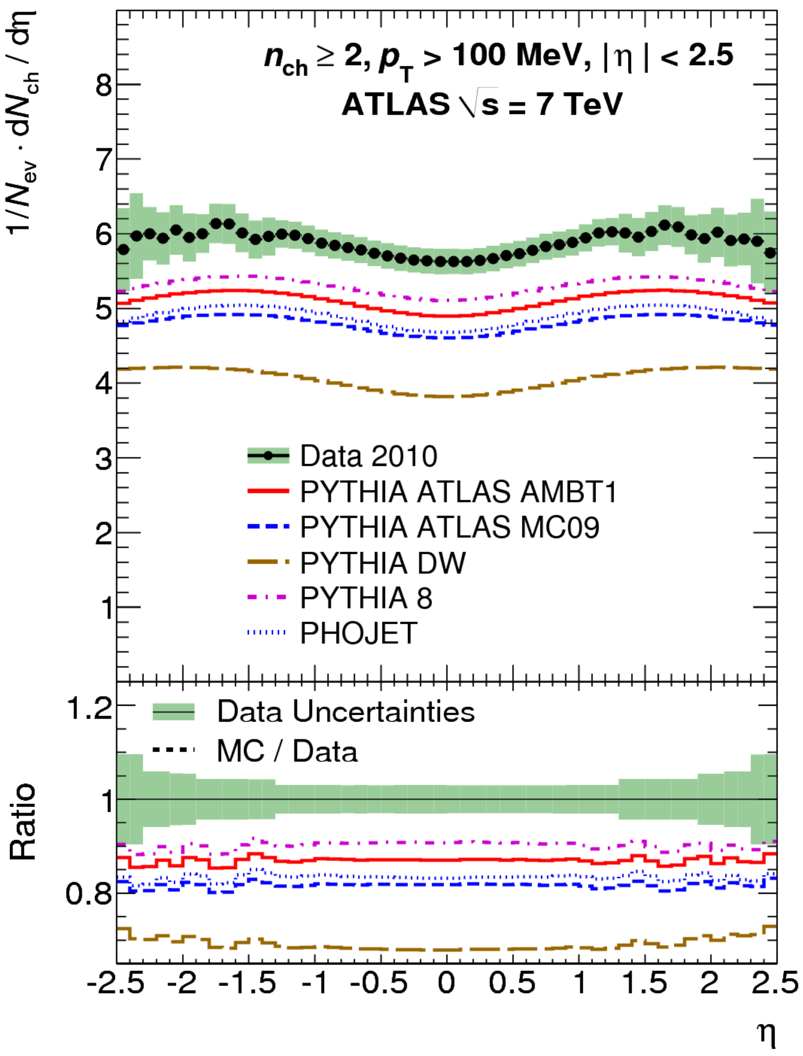

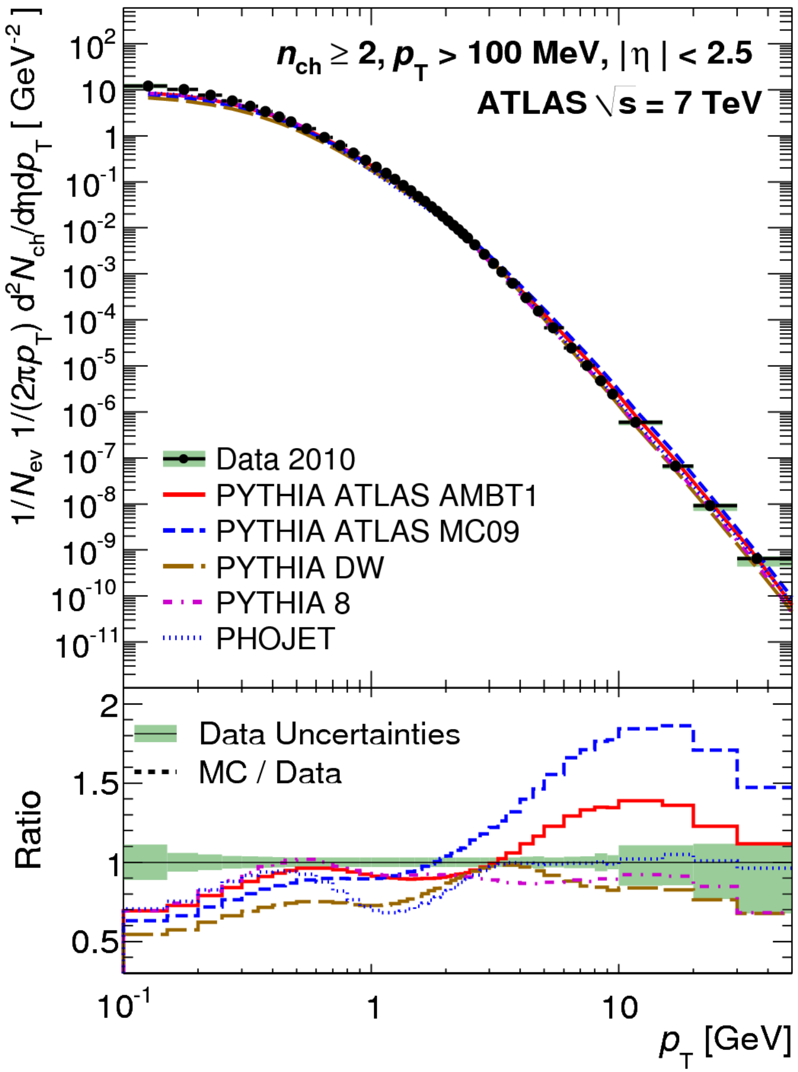

dN_{ev}/dn_{ch}

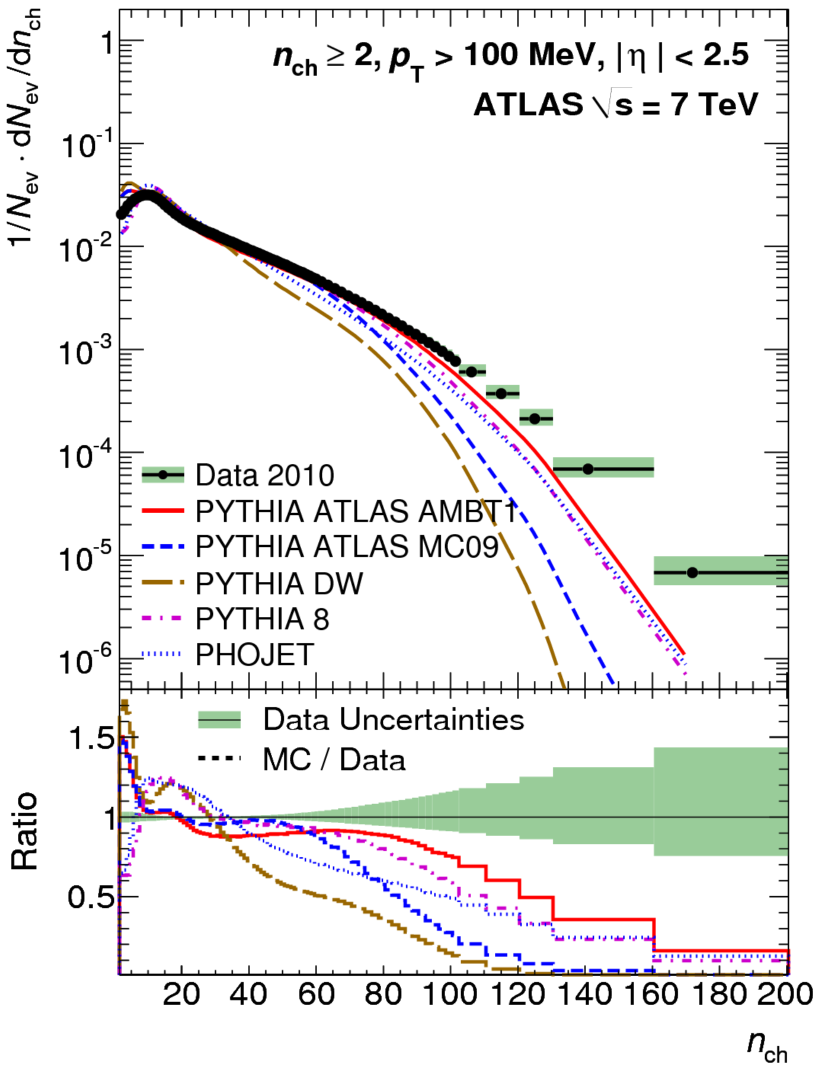

<p_T> vs n_{ch}

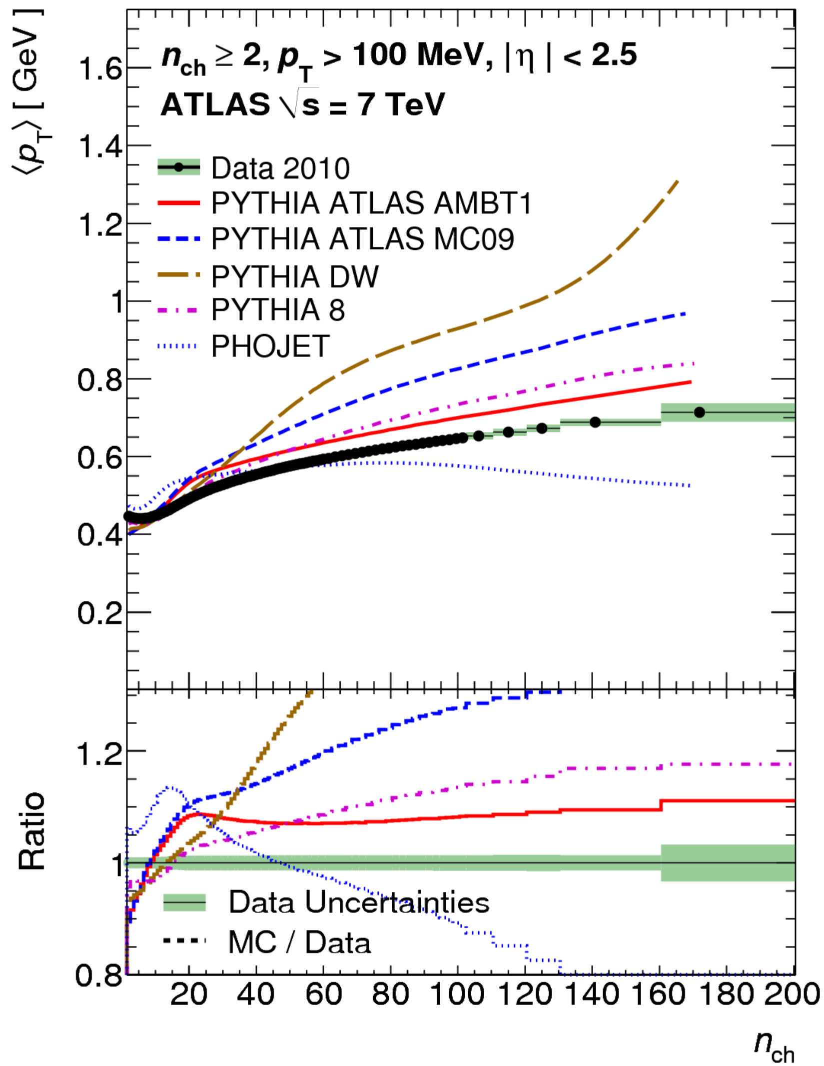

$dN_{ch}/d\eta$ at $\eta = 0$ vs $\sqrt{s}$

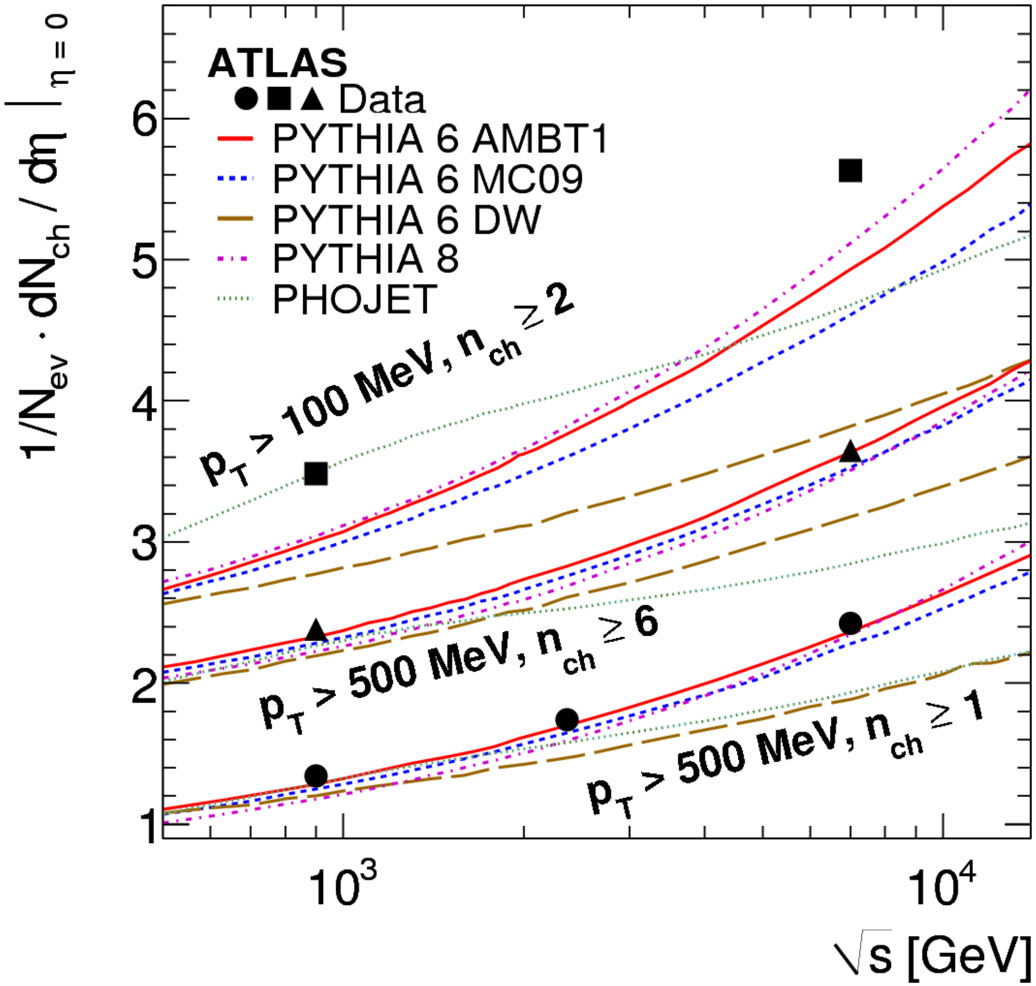

W production

- The W (and Z) boson production expected from the Standard Model is an important background for top quark production and for searches beyond the standard model.
- W (and Z) bosons provide a source of high p_T isolated leptons.
  - Used to understand detector and trigger performance, lepton identification and MET resolution.
- Inclusive and associated jets analyses have been carried out.

Electron identification

- Electrons are selected with three levels of selection, each tighter than the first.
- The definition of these selection criteria depends on ongoing optimisation.
- Typically:
  - The loosest selection is based on transverse and longitudinal shower shape in the second layer of the calorimeter, with a requirement on the hadronic leakage.
  - A slightly more robust selection is given by using shower shape measurements in the first layer of the calorimeter and track quality and impact parameter
  - The most robust requirement uses cluster-track energy vs momentum, transition radiation in the TRT, at least one pixel b-layer hit.

Muon identification

- Stand-alone muon-spectrometer track associated to an inner-detector track.
  - association found from best χ^2
  - combine tracks or refit.
  - W+jets and Top analysis use additional track quality, matching and impact parameter requirements.
    - Further reduce QCD background.

QCD background

- All other source of background not included in another term.
  - Jets which deposit a lot of energy in the electromagnetic calorimeter
  - Conversions in material before first pixel layer.
  - Muons produced from long lived weakly decaying particles.
- Tightly coupled to the detector description and the result of fluctuations.
  - Create templates from adjacent control regions, where signal is ≈ 0.
  - Use looser selection and calculate:

$$
\begin{aligned}
N_{\mathrm{loose}} &= N_{\mathrm{nonQCD}} + N_{\mathrm{QCD}} \\
N_{\mathrm{iso}} &= \varepsilon^{\mathrm{iso}}_{\mathrm{nonQCD}} N_{\mathrm{nonQCD}} + \varepsilon^{\mathrm{iso}}_{\mathrm{QCD}} N_{\mathrm{QCD}}
\end{aligned}
$$

solving for N_{QCD} given the two efficiency factors.

W inclusive: event selection

- Presence of a primary vertex
- Electron ET > 20 GeV or combined muon p_T > 20 GeV
- Muon isolation $\Sigma p_T^{ID}/p_T < 0.2$ within $\Delta R < 0.2$

$$\Delta R = \sqrt{\Delta\phi^2 + \Delta\eta^2}$$

- ETmiss > 25GeV
- m_T > 40GeV, where the transverse mass is:

$$m_{\mathrm{T}} = \sqrt{2\, p_{\mathrm{T}}^{\ell}\, E_{\mathrm{T}}^{\mathrm{miss}}\, (1 - \cos\Delta\phi)}$$

and Δφ is the azimuthal separation between ETmiss and the lepton.

W inclusive: fiducial limits

- $W \rightarrow e\nu$
  - ETe > 20 GeV
  - $|\eta_e| < 2.47$, excluding $1.37 < |\eta_e| < 1.52$
  - $p^\nu_T > 25$ GeV
  - $m_T > 40$ GeV
- $W \rightarrow \mu\nu$
  - $p^\mu_T > 20$ GeV
  - $|\eta_\mu| < 2.4$
  - $p^\nu_T > 25$ GeV
  - $m_T > 40$ GeV

W→$\mu\nu_\mu$ inclusive: p_T & m_T

Muon candidate events and backgrounds before ETmiss requirement

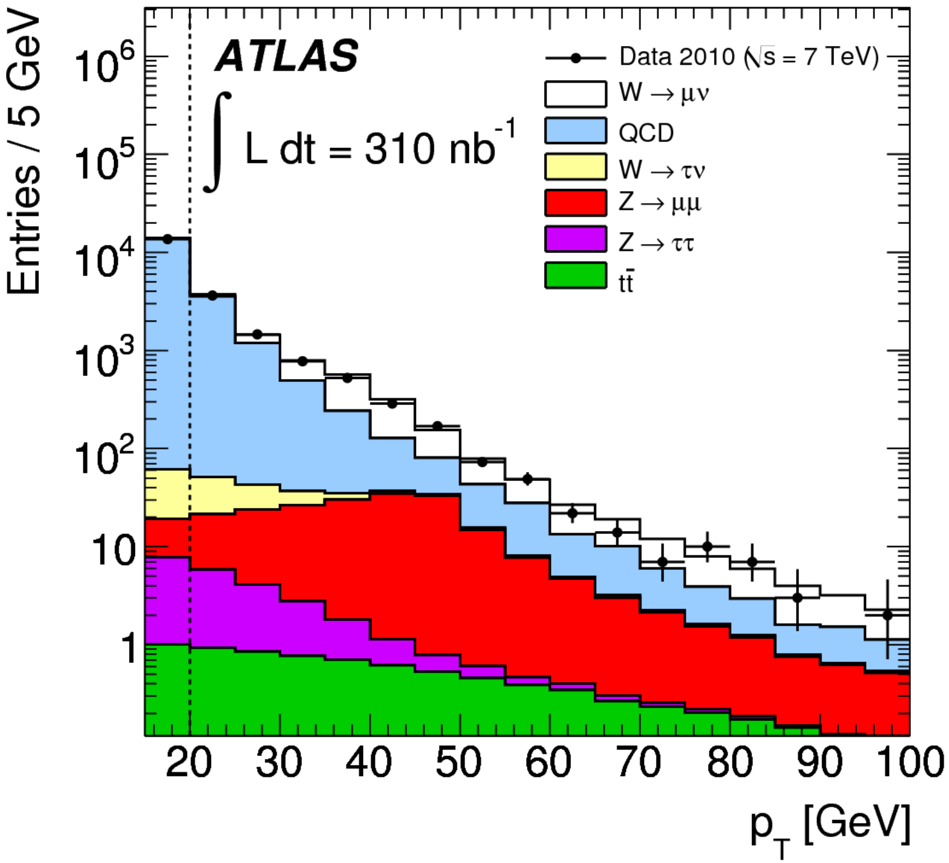

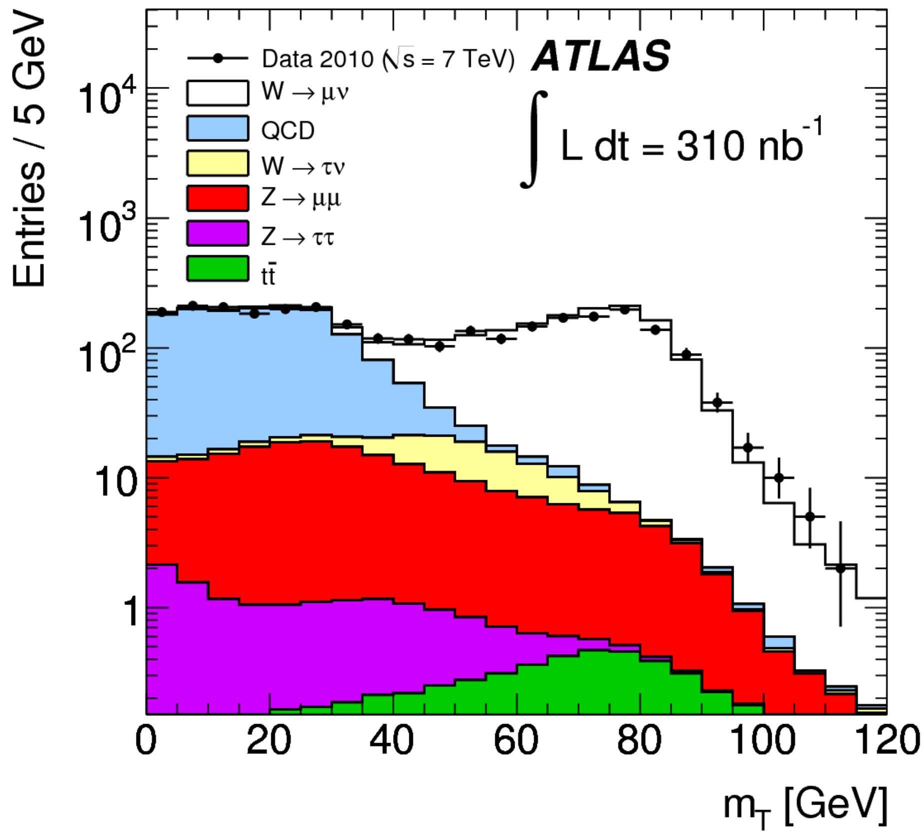

W→μν$_\mu$ inclusive: m_T & p_T

Muon candiate events and backgrounds

After ETmiss > 25GeV

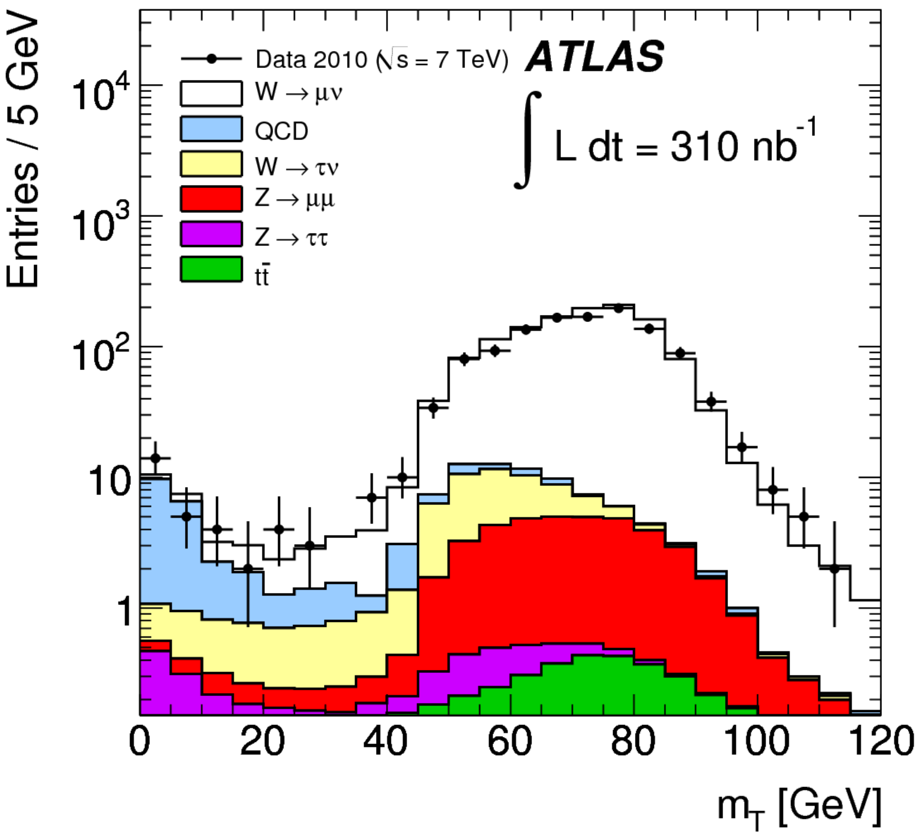

After ETmiss > 25GeV & m_T > 40GeV

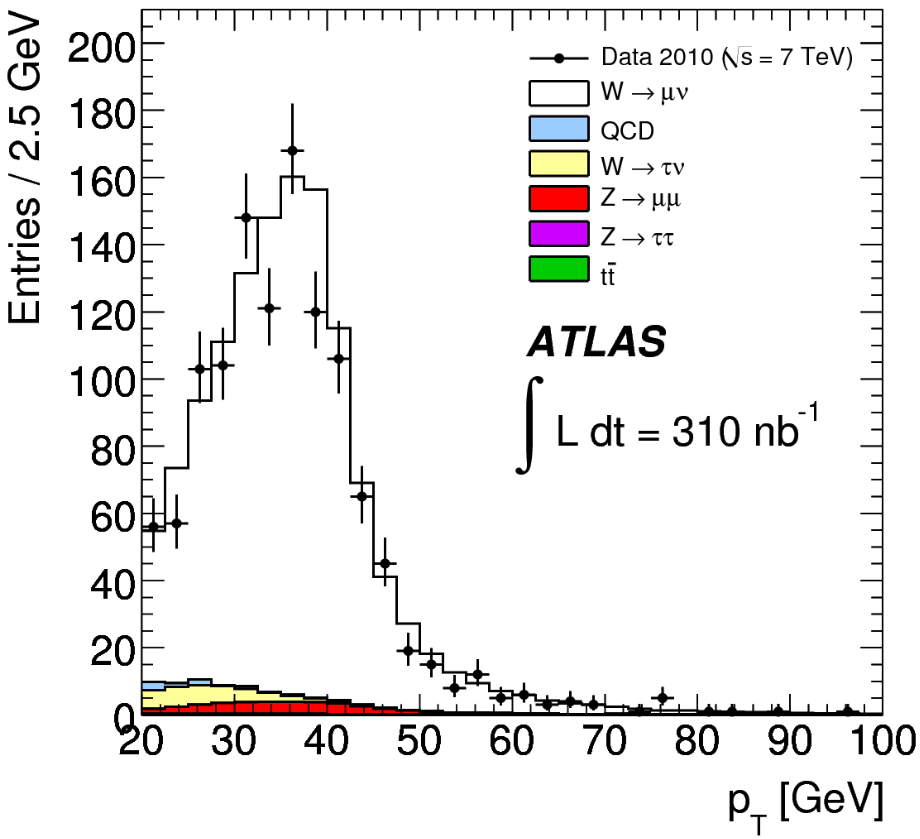

$W \rightarrow \mu\nu_\mu$ inclusive: candidates and backgrounds

ℓ	Observed candidates	Background (EW+$t\bar{t}$)	Background (QCD)	Background-subtracted signal N_W^{sig}
e^+	637	$18.8 \pm 0.2 \pm 1.7$	$14.0 \pm 2.1 \pm 7.1$	$604.2 \pm 25.2 \pm 7.6$
e^-	432	$14.7 \pm 0.2 \pm 1.3$	$14.0 \pm 2.1 \pm 7.1$	$403.2 \pm 20.8 \pm 7.5$
$e^\pm$	1069	$33.5 \pm 0.2 \pm 3.0$	$28.0 \pm 3.0 \pm 10.0$	$1007.5 \pm 32.7 \pm 10.8$
μ^+	710	$42.5 \pm 0.2 \pm 2.9$	$12.0 \pm 3.0 \pm 4.6$	$655.6 \pm 26.6 \pm 6.2$
μ^-	471	$35.1 \pm 0.2 \pm 2.4$	$10.9 \pm 2.4 \pm 4.1$	$425.0 \pm 21.7 \pm 5.4$
$\mu^\pm$	1181	$77.6 \pm 0.3 \pm 5.4$	$22.8 \pm 4.6 \pm 8.7$	$1080.6 \pm 34.4 \pm 11.2$

Electroweak backgrounds ($W \rightarrow \tau\nu$, $Z \rightarrow ll$, $Z \rightarrow \tau\tau$)

The background-subtracted signal events are used to calculate fiducial cross sections.

σ_W x BR(W→lν) for W+, W-

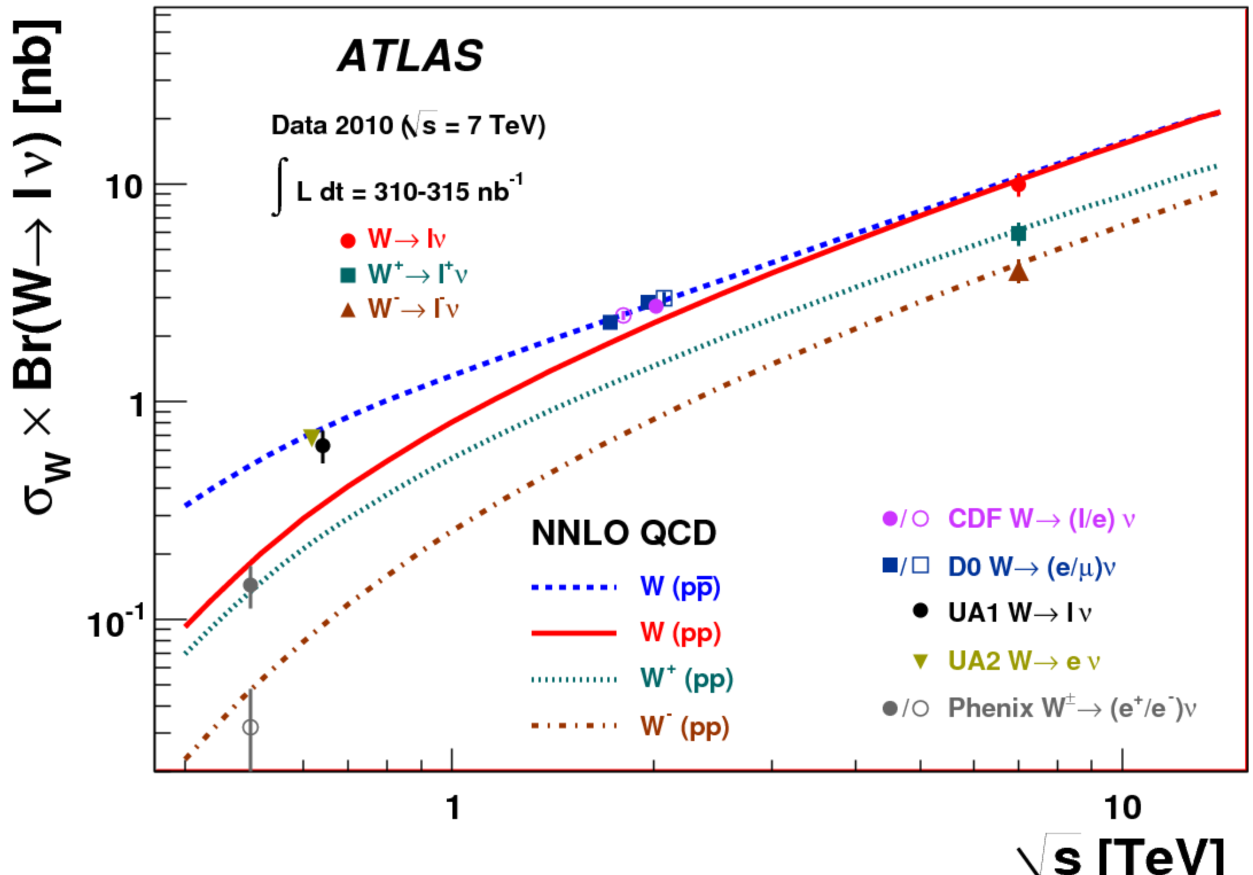

MC derived acceptance factors are used to convert the fiducial cross-section results into cross sections for the full phase space.

The W+/W- production asymmetry is expected from the u and d quark distributions in the proton.

W production asymmetry

$$A_\ell = \frac{\sigma^{\mathrm{fid}}_{W^+} - \sigma^{\mathrm{fid}}_{W^-}}{\sigma^{\mathrm{fid}}_{W^+} + \sigma^{\mathrm{fid}}_{W^-}}$$

Used to constrain parton distribution functions.

Expected from u and d valence quark distributions in the proton.

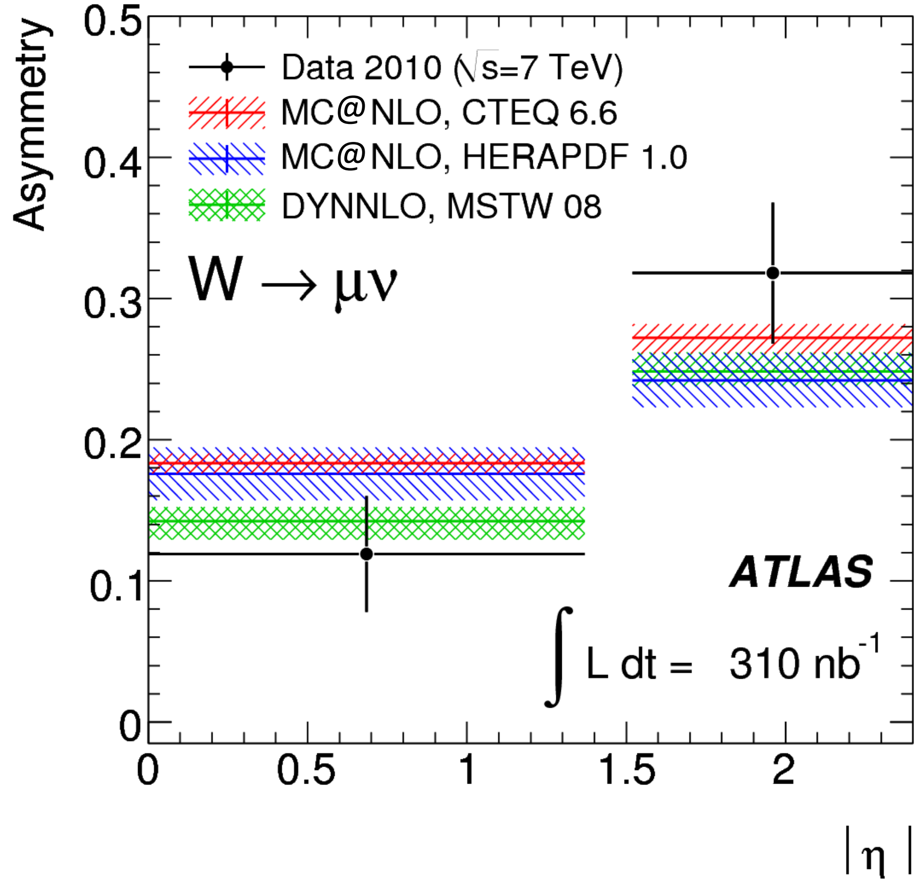

Uncertainty bounds correspond to 90% CL on PDF sets.

$\sigma_W / \sigma_{Z\gamma^*}$

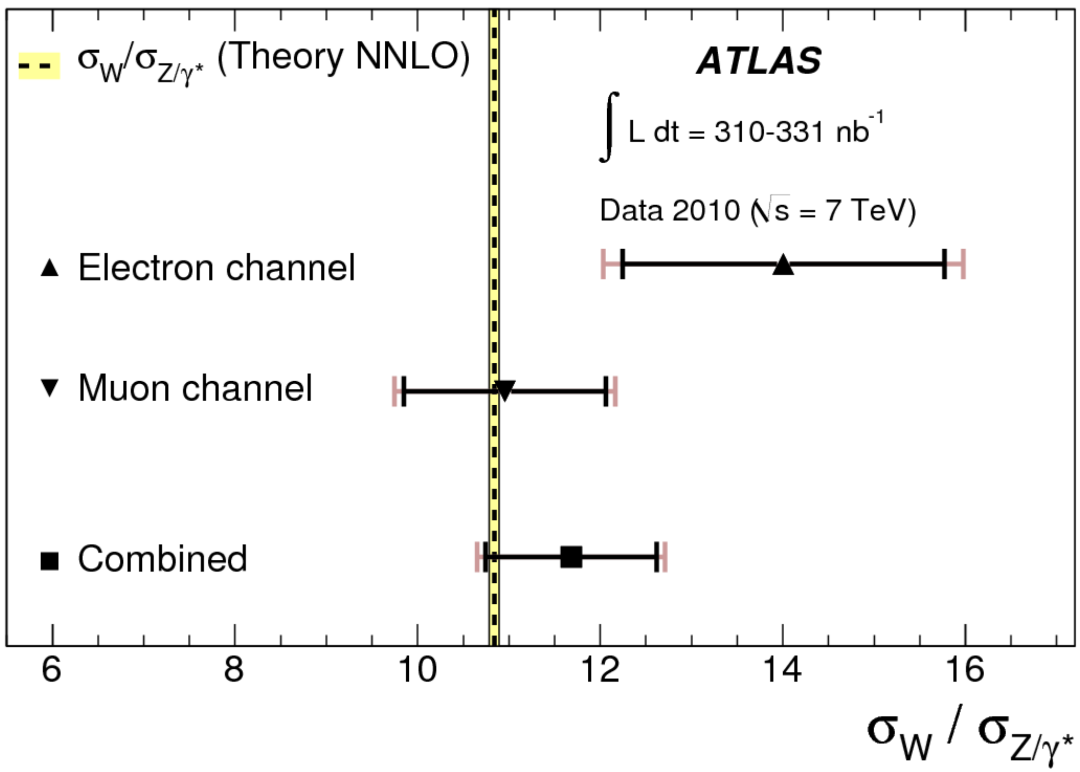

Experimental and theoretical uncertainties partially cancel to provide a more powerful test of the standard model.

W+jets production cross-section

- Test QCD as a function of the number of jets and the leading jet p_T.
- Important background for ttbar, Higgs and BSM physics.

- Very similar selection to the inclusive W analysis.
  - Some additional requirements were made in the muon identification to reduce the QCD background.

W+jets: associated jet multiplicities

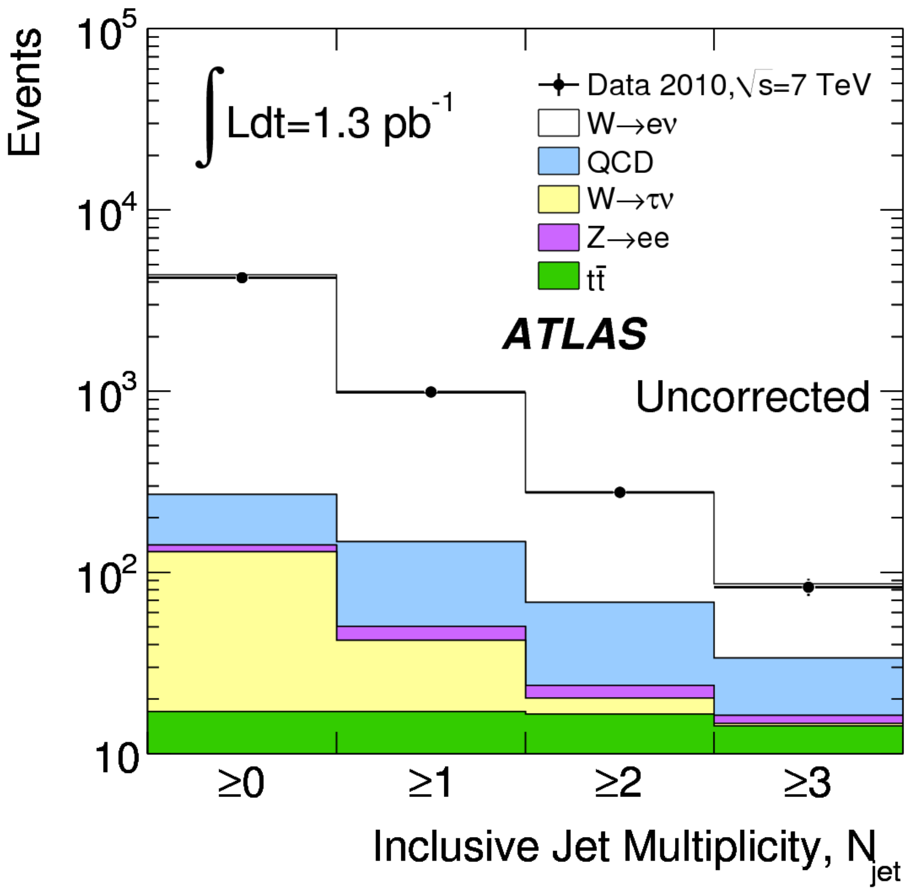

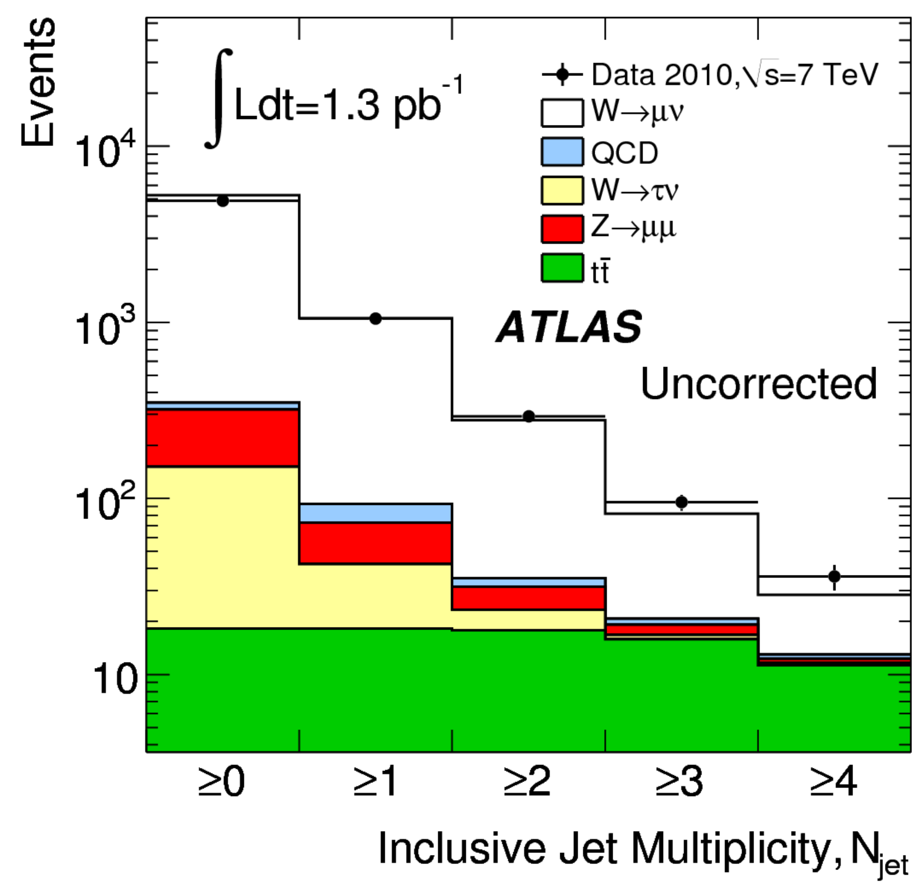

W+jets: fiducial limits

- In a similar manner to the inclusive W measurements the cross-section is quoted within a fiducial limit corresponding to the detector acceptance and event selection at the particle-level.
  - $ET_j > 20$ GeV, $|\eta_j| < 2.8$,
  - $ET_l > 20$ GeV
  - $|\eta_e| < 2.47$ (excluding $1.37 < |\eta_e| < 1.52$)
  - $|\eta_\mu| < 2.4$
  - $p^{\nu}_T > 25$GeV, $m_T >40$GeV, $\Delta R_{lj} >0.5$

W+jets: inclusive jet multiplicity

Measurements at the particle-level, within the selected fiducial volume.

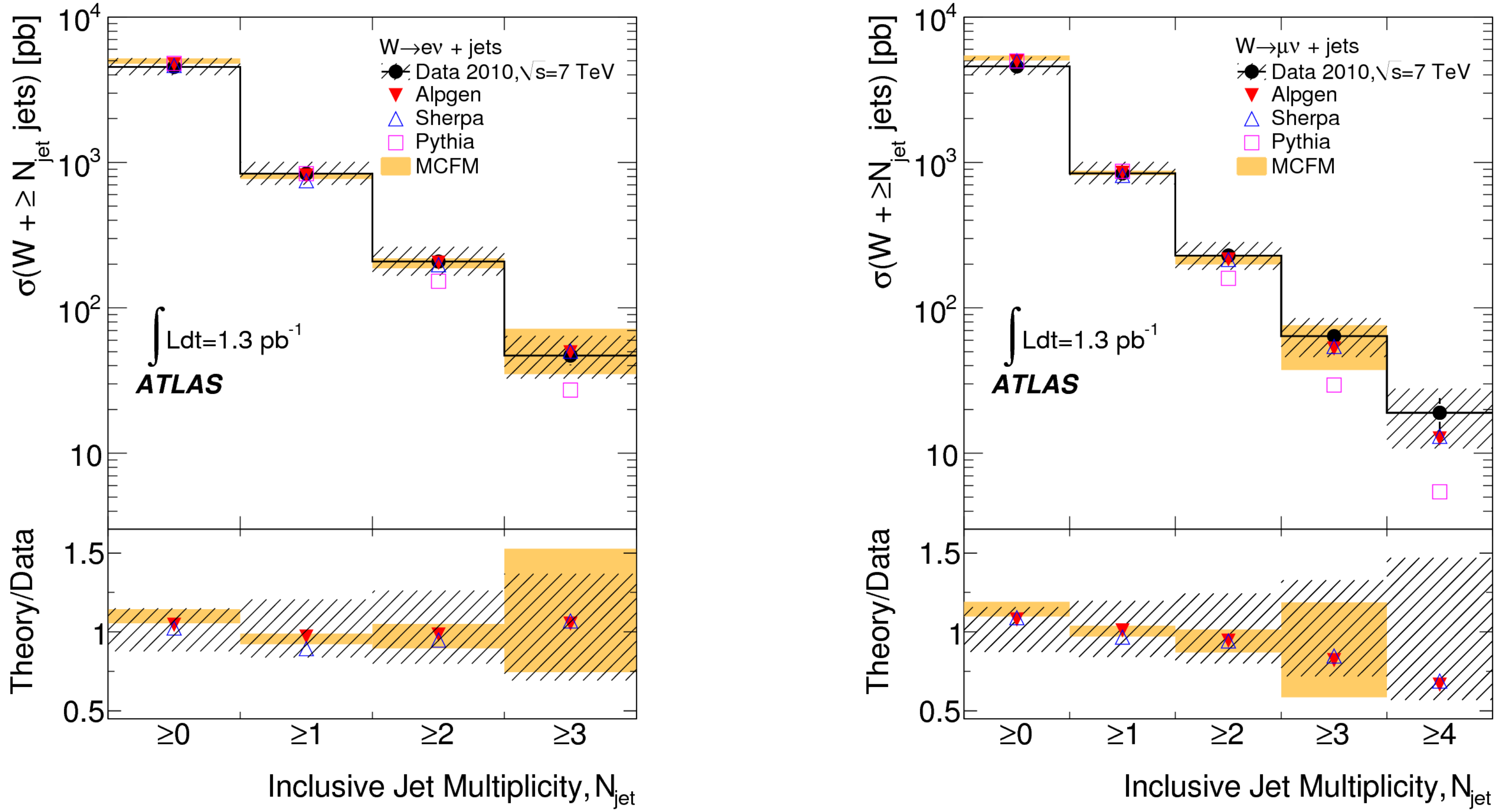

Measurements at the particle-level, within the selected fiducial volume.

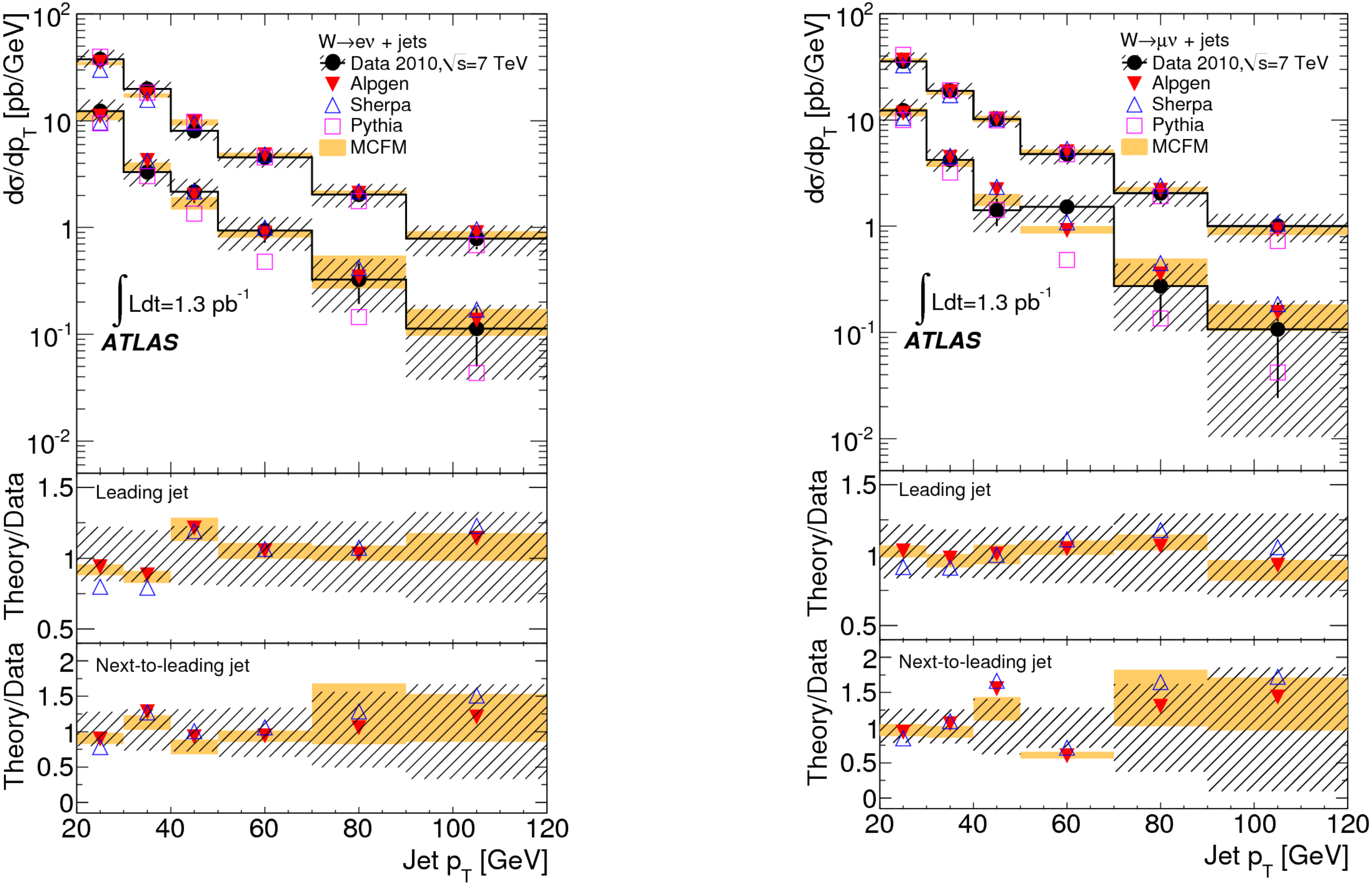

The top quark

- The heaviest fundamental particle observed.
  - Expect large coupling to the mediator of electroweak symmetry breaking.
  - Possible new physics may couple to the top quark.
    - Therefore, seek to test Standard Model predictions of properties and production.

b-tagging

50% working point

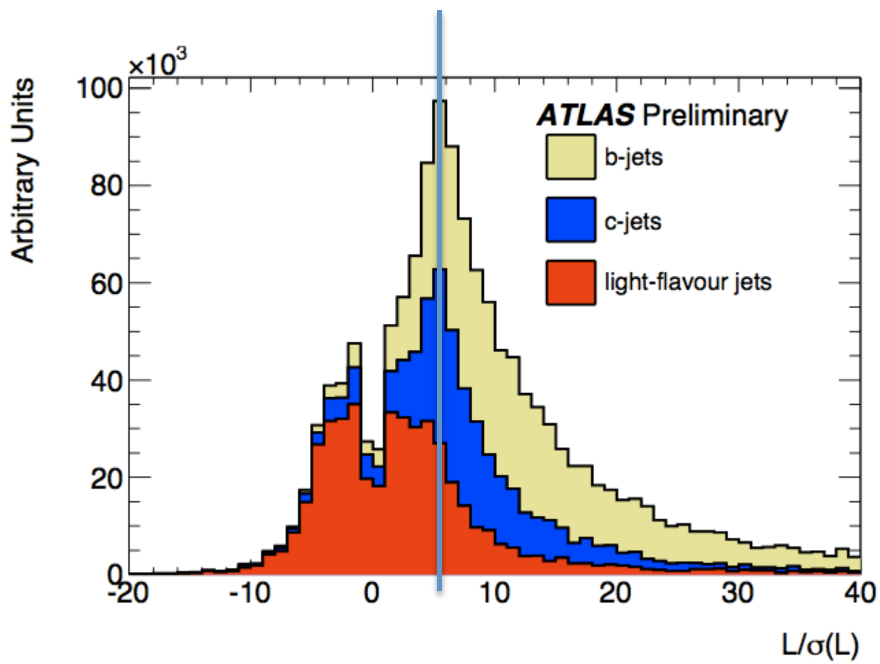

The signed decay length significance $L/\sigma(L)$ for the SV0 *b*-tagging algorithm for simulated QCD jets

- Tracks associated with a jet are used to determine the decay length of the particle which fragmented into a jet.
  - Tracks are chosen that fulfill minimal quality requirements.
  - A secondary vertex fit is formed iteratively removing tracks with large χ^2 contributions until the χ^2 of the fit is below a selected threshold.
  - Two track vertices which originate from a material layer are discarded.

Top (l+jets): event selection

- Similar lepton identification to the W+jets analysis.
- Exclusively one lepton with $p_T > 20$GeV
- ETmiss > 20 GeV
- ETmiss + $m_T > 60$ GeV
- Jet $p_T > 25$ GeV
- One or more b-tagged jet. (“tagged”)

Jet multiplicity distributions

For jets with p_T > 25 GeV & |η| < 2.5

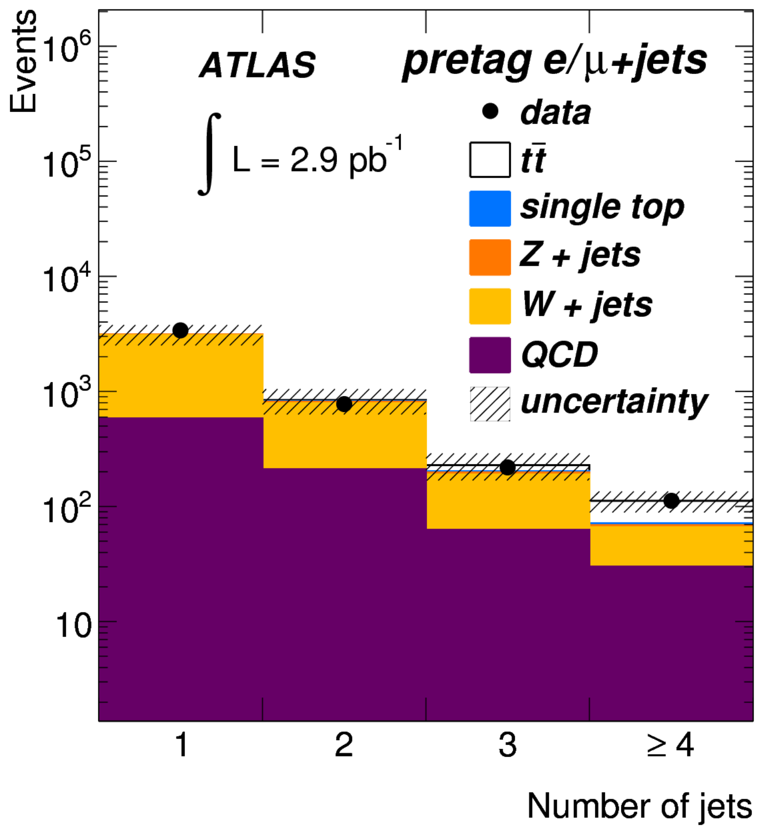

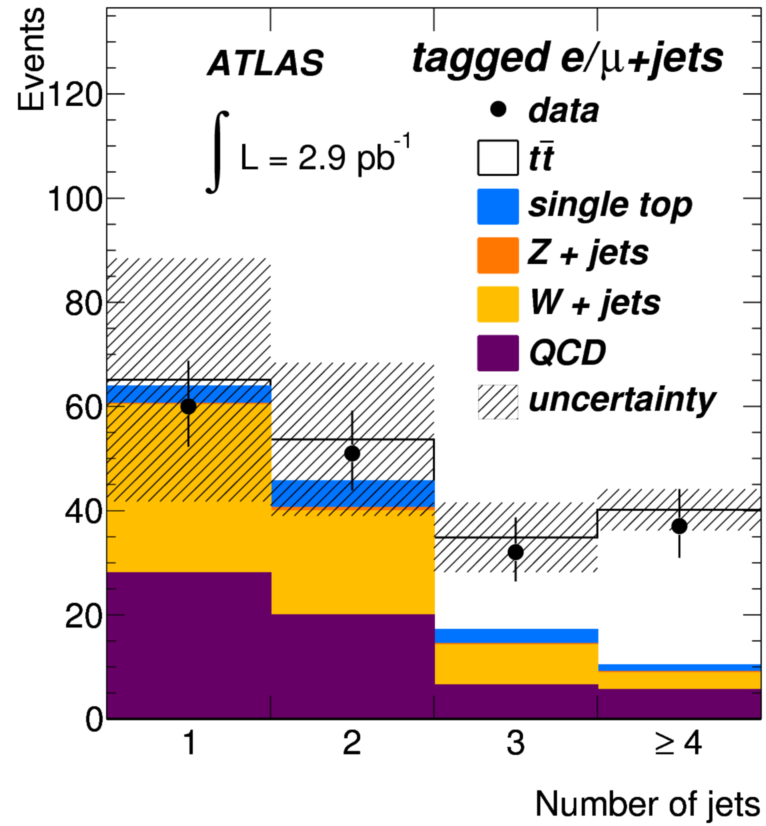

Hatched area represents total uncertainty on background.

M_{jjj} invariant mass

Hardest three jets are combined without b-tagging weight. The combination is ~25% correct. There is good agreement between predicted and observed ttbar shapes.

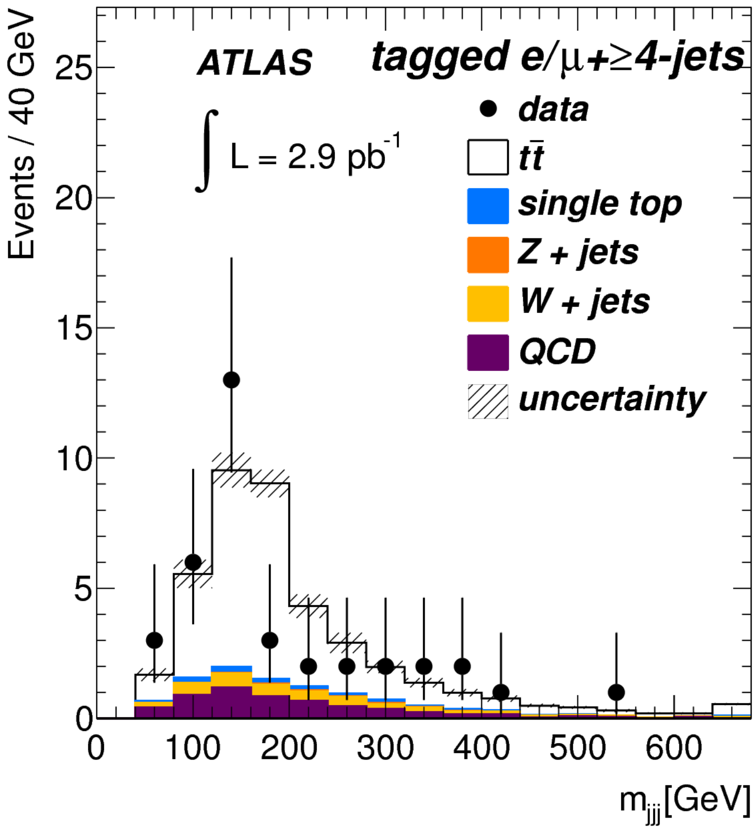

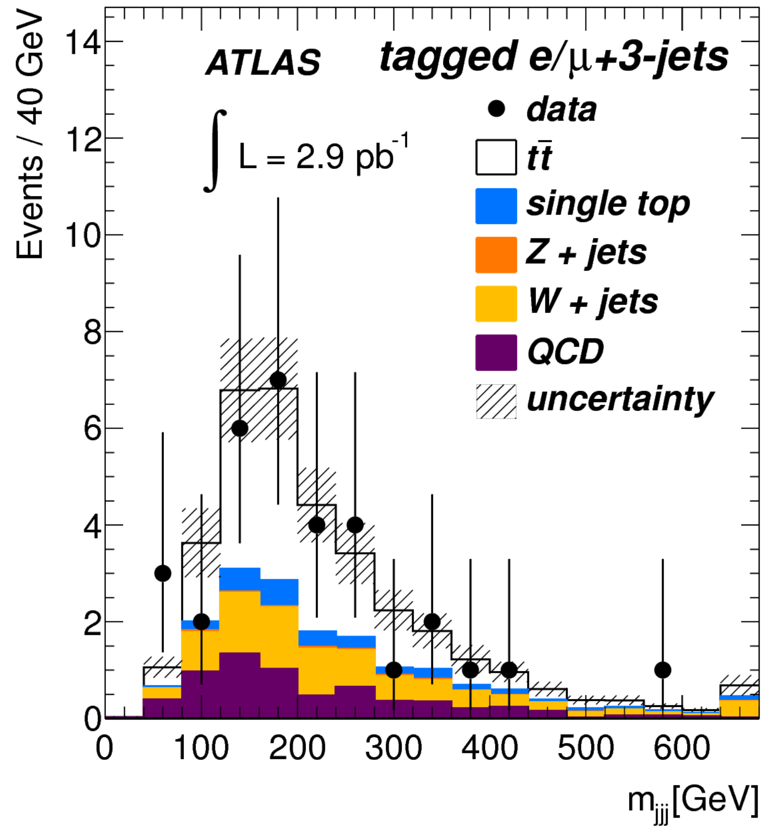

Hatched area represents total uncertainty on background.

Forming a final result

- The number of events in the inclusive 4 jet bin after background subtraction was used together with acceptance factors derived from MC and the branching ratios
- The result of the l+jets analysis was combined with the di-lepton analysis to form a final result.

First ttbar cross-section comparison

ATLAS result is from a combination of l+jets and dilepton
CMS result is from just the dilepton channels

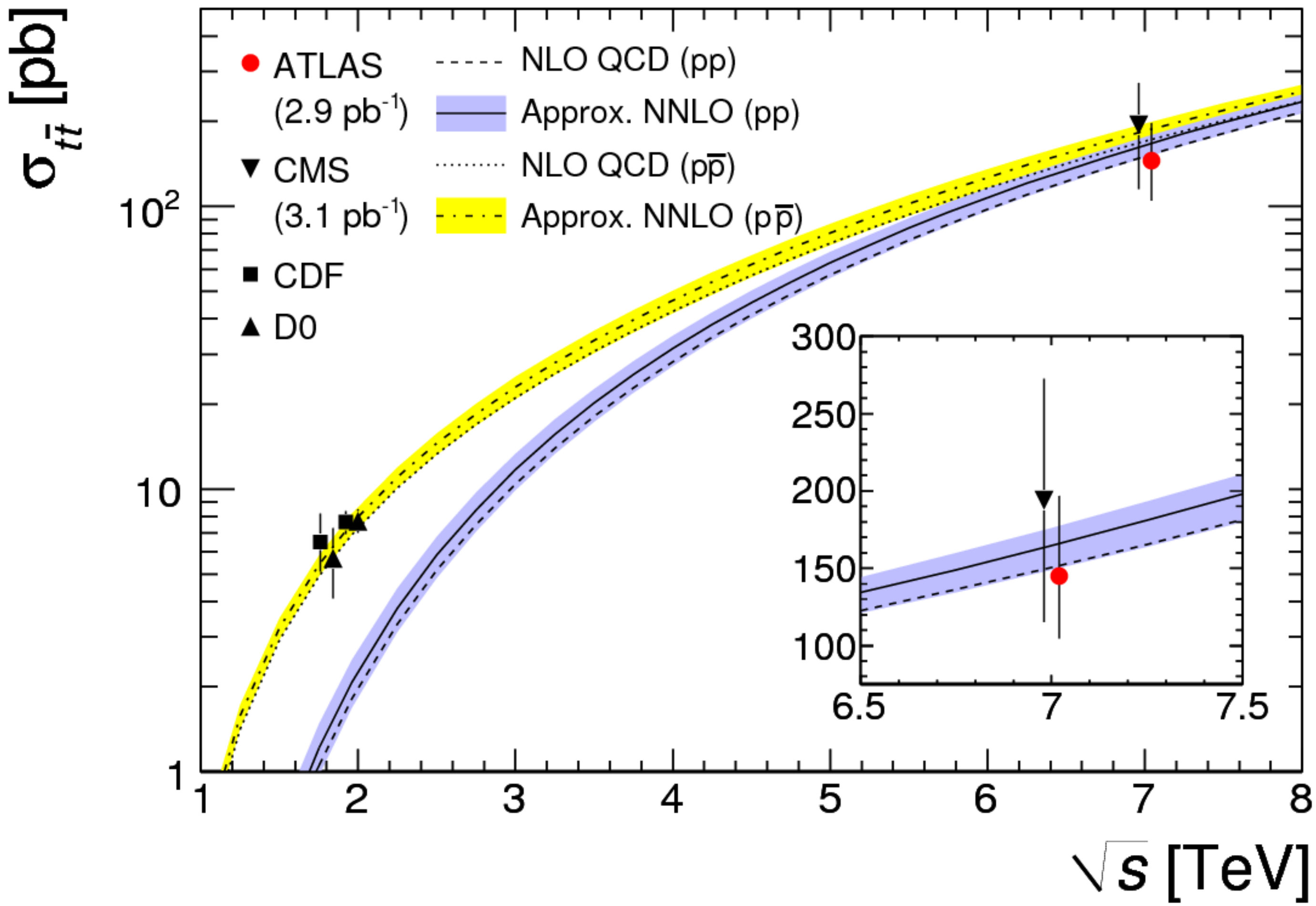

Conclusions

- Charged-particle multiplicity studies have lead to better MC tunes.
  - Diffractive models could still be improved.
- Inclusive W and W with associated jet production cross-sections have been measured.
  - Perturbative QCD calculations agree with these measurements.
- An initial ttbar cross-section measurement has been made.
  - CMS and ATLAS results are in agreement.
  - NNLO QCD measurements agree with these measurements.

Analyses for 2011/12

- Production cross-section of ttbar + jets
  - Experimental measurements of 0 and 1 jet at the Tevatron.
  - Theoretical calculations are difficult.
    - Large number of diagrams and the presence of massive particles.
  - Background to Higgs boson production in vector boson fusion, BSM processes involving lepton + jets.
- t' – Heavy top like 4th generation searches.
- ttbar production asymmetry
  - 2σ excess observed at the Tevatron.
- Vector boson scattering (W+jets, Z+jets)
  - Discriminate between Higgs and dynamic symmetry breaking models.

ttbar, associated jets and asymmetry

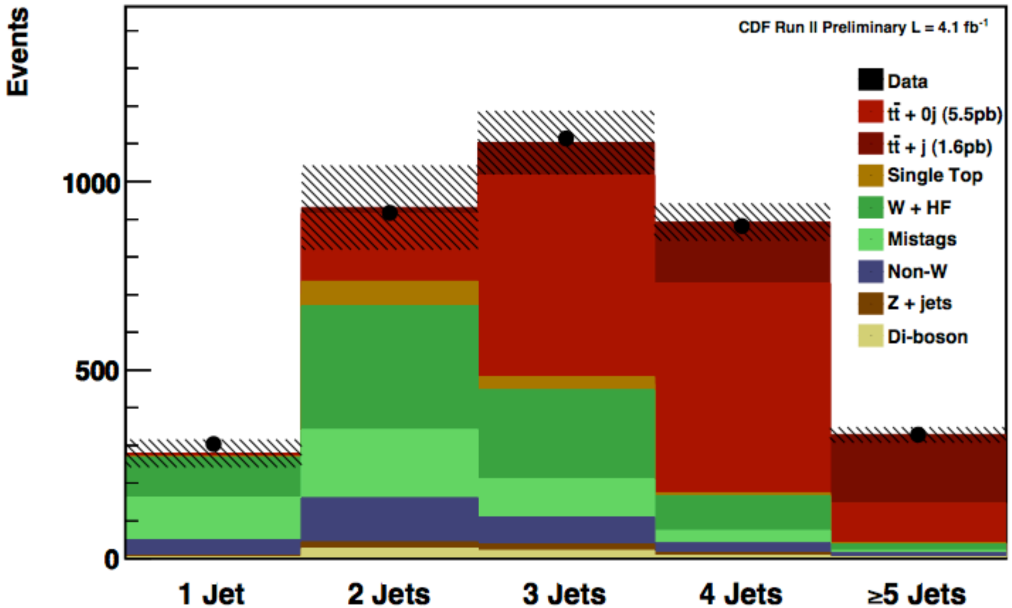

Expected and observed number of events as a function of jet multiplicity for events with at least one b-tag and additional selection

H_T > 220 GeV, and MET > 20 GeV

Inclusive forward-backward asymmetry in tt production in the dilepton channel using 334 dilepton candidates

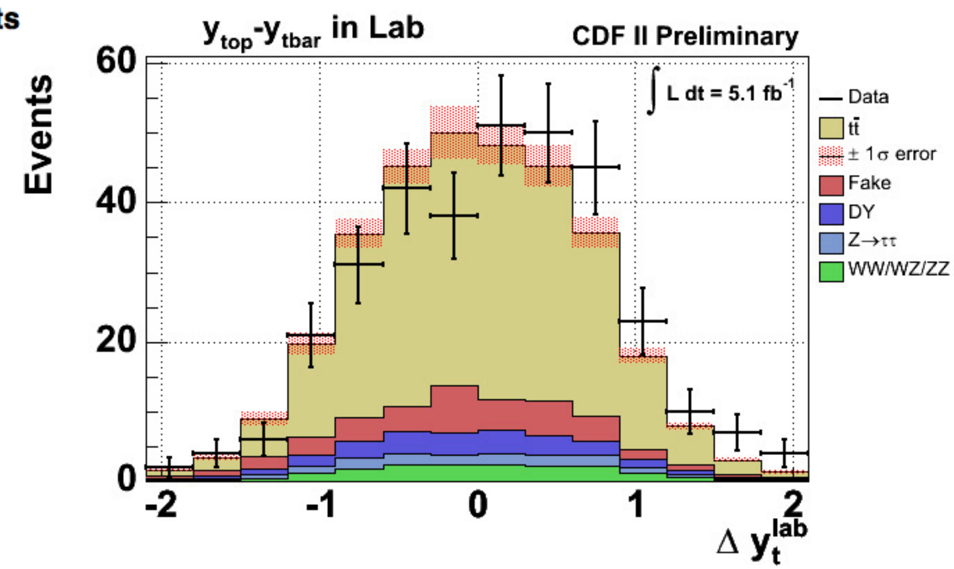

References for further reading

arXiv:1012.5104 Charged-particle multiplicities

arXiv:1010.2130 Inclusive W cross-section

arXiv:1012.5382 W+jets cross-section

arXiv:1012.1792 Top cross-section

Additional slides

Charged-particle multiplicities

Systematic Uncertainty	Size	Region
Material	$\pm 2 - 15\%$	decreases with p_{T}, increases with $\lvert\eta\rvert$
χ^2 prob. cut	$\pm 10\%$	flat, only for $p_{\mathrm{T}} > 10$ GeV
Resolution	$\pm 5\%$ negligible -7%	$100 < p_{\mathrm{T}} < 150$ MeV $0.15 < p_{\mathrm{T}} < 10$ GeV $p_{\mathrm{T}} > 10$ GeV
Track Selection	$\pm 1\%$	flat in p_{T} and η
Truth Matching	$\pm 1\%$	only for $\sqrt{s} = 2.36$ TeV Pixel Tracks
Efficiency correction factor	$\pm 4\%$	only for $\sqrt{s} = 2.36$ TeV ID Track
Alignment and other high p_{T}	-3% to -30%	only for $p_{\mathrm{T}} > 10$ GeV averaged over η, increases with increasing p_{T}

Table 5: The systematic uncertainties on the track reconstruction efficiency for $\sqrt{s} = 0.9$ TeV, $\sqrt{s} = 7$ TeV and $\sqrt{s} = 2.36$ TeV Pixel Track and ID Track methods. Unless otherwise stated, the systematic is similar for all energies and phase-space regions. All uncertainties are quoted relative to the track reconstruction efficiency.

LAr calorimeter module

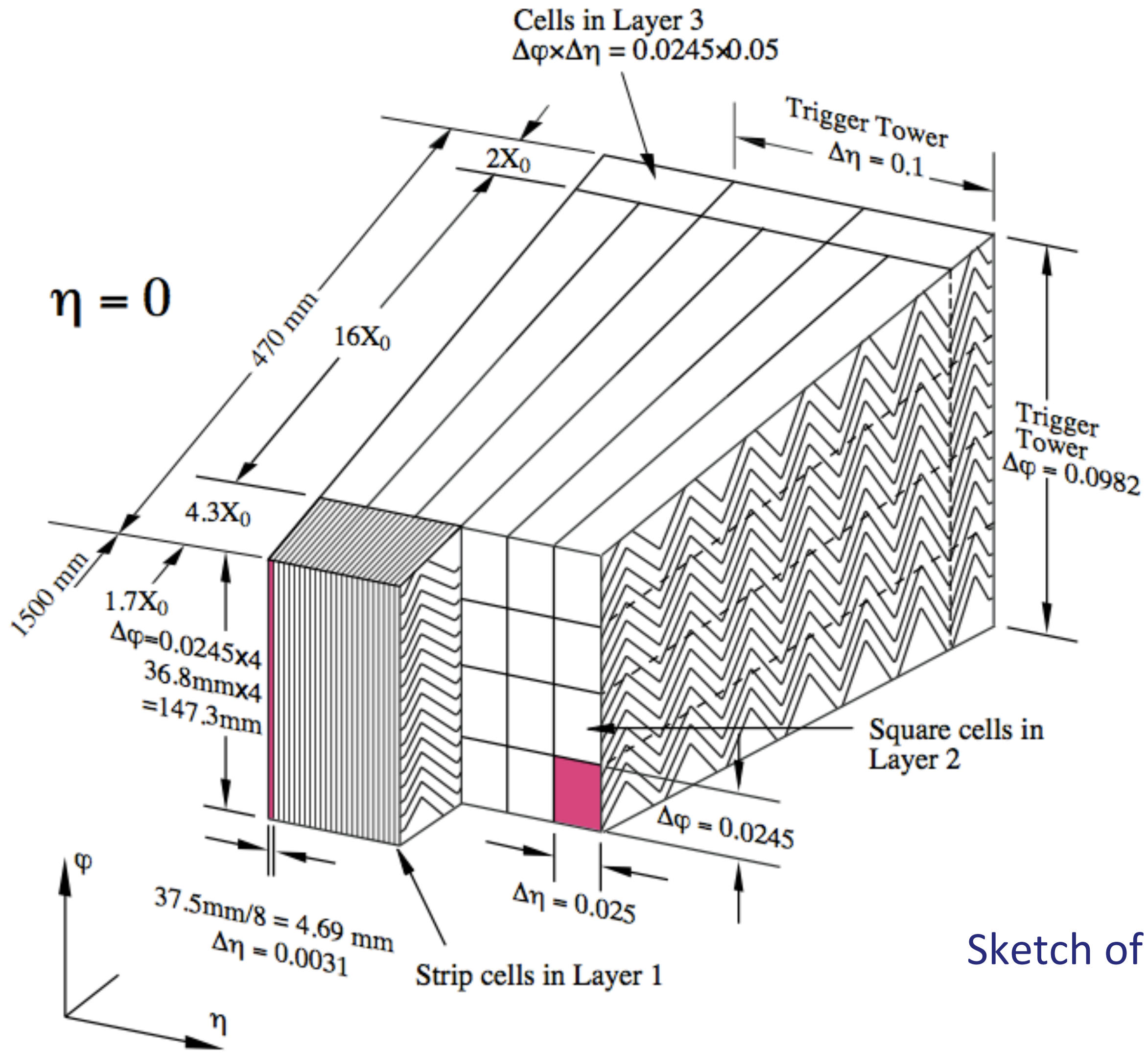

Sketch of a barrel module

σ_W x BR(W→lν) for W+, W-

$$\sigma^{\text{tot}}_{W^+} \cdot \mathrm{BR}(\mathrm{W} \rightarrow \ell\nu) = 5.93 \pm 0.17\,(\text{stat}) \pm 0.30\,(\text{syst}) \pm 0.65\,(\text{lumi})\ \text{nb},$$

$$\sigma^{\text{tot}}_{W^-} \cdot \mathrm{BR}(\mathrm{W} \rightarrow \ell\nu) = 4.00 \pm 0.15\,(\text{stat}) \pm 0.20\,(\text{syst}) \pm 0.44\,(\text{lumi})\ \text{nb},$$

$$\sigma^{\text{tot}}_{W} \cdot \mathrm{BR}(\mathrm{W} \rightarrow \ell\nu) = 9.96 \pm 0.23(\text{stat}) \pm 0.50(\text{syst}) \pm 1.10(\text{lumi})\ \text{nb}.$$

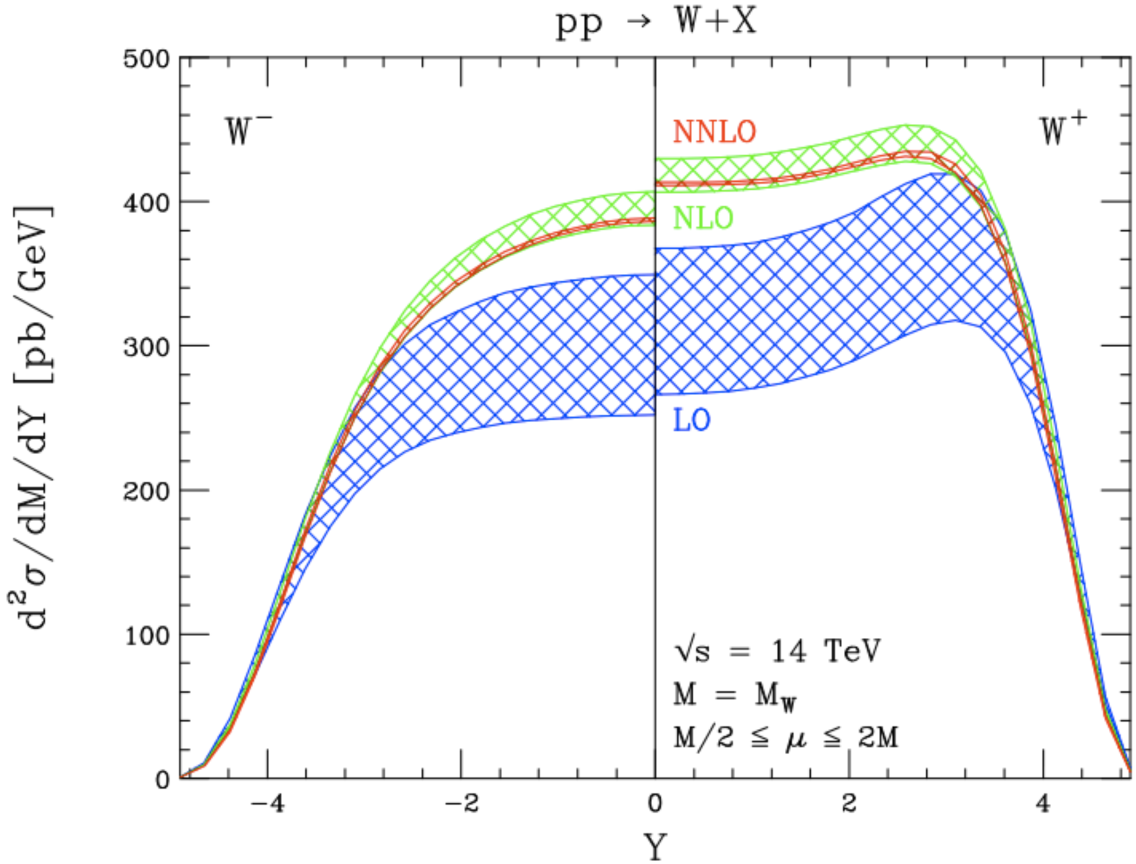
pp → W+X
W⁻
W⁺
NNLO
NLO
LO
√s = 14 TeV
M = M_W
M/2 ≤ μ ≤ 2M
d²σ/dM/dY [pb/GeV]
Y

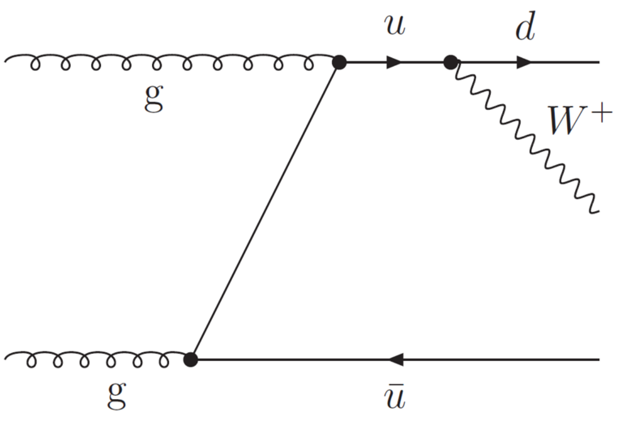
g
u
d
W⁺
g
ū

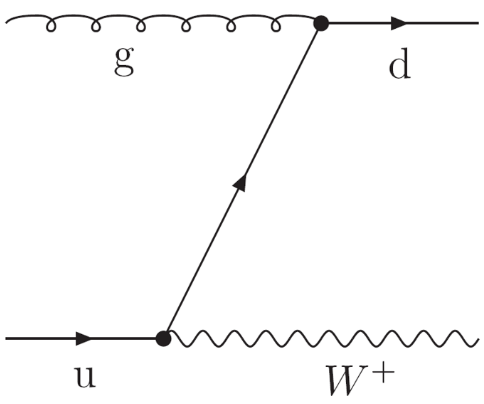
g
d
u
W⁺

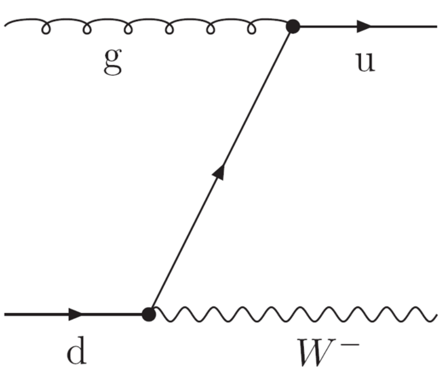
g
u
d
W⁻

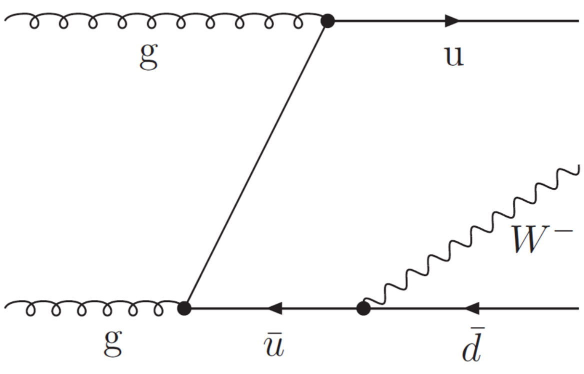
g
u
W⁻
g
ū
d̄

W+jets systematic uncertainties

e channel		
Effect	Range	Cross Section Uncertainty (%)
Jet energy scale and E_T^{miss}	$\pm 10\%$ (dependent on jet η and p_T) $\oplus$ 5%	+11, -9
Jet energy resolution	14% on each jet	± 1.0
Electron trigger	$\pm 0.5\%$	∓ 0.7
Electron identification	$\pm 5.2\%$	∓ 5.5
Electron energy scale	$\pm 3\%$	+3.9, -4.7
Pile–up removal cut	$4-7\%$ in lowest jet p_T bin	± 1.9
Residual pile-up effects	from simulation	± 2.2
QCD background shape	from template variation	-1.5, +5.2
Luminosity	$\pm 11\%$	-10, +13

μ channel		
Effect	Range	Cross Section Uncertainty (%)
Jet energy scale and E_T^{miss}	$\pm 10\%$ (dependent on jet η and p_T) $\oplus$ 5%	+11, -9
Jet energy resolution	14% on each jet	± 1.8
Muon trigger	$\pm 2.5\%$ in barrel, $\pm 2.0\%$ in endcap	∓ 1.6
Muon reconstruction	$\pm 5.6\%$	-5.4, +5.9
Muon momentum scale	$\pm 1\%$	+2, -0.9
Muon momentum resolution	$\pm 5\%$ in barrel, $\pm 9\%$ in endcap	± 1.4
Pile–up removal cut	$4-7\%$ in lowest jet p_T bin	± 1.7
Residual pile-up effects	from simulation	± 1.4
Luminosity	$\pm 11\%$	-11, +13

Table 3: Summary of the systematic uncertainties in the cross section. The uncertainties are shown only for $N_{jet} \geq 1$. The sign convention for the JES and lepton energy scale uncertainties is such that a positive change in the energy scale results in an increase in the jet or lepton energy observed in the data.

b-tagging

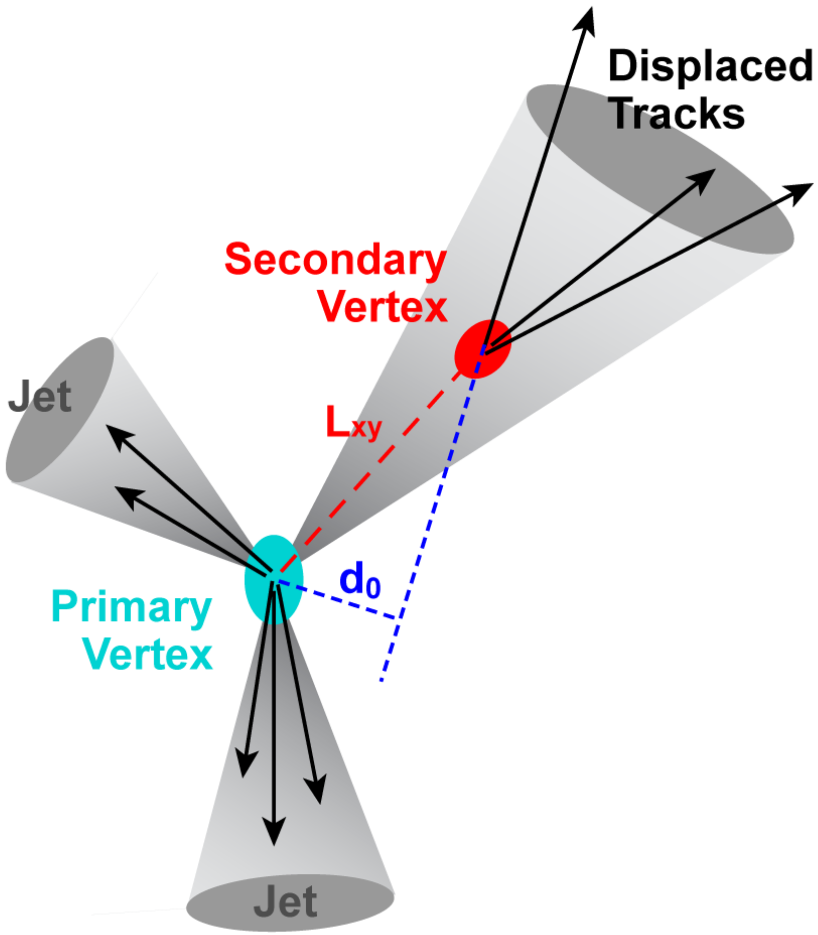
Displaced
Tracks
Secondary
Vertex
Jet
L_{xy}
d_0
Primary
Vertex
Jet

ttbar cross-section: uncertainties

	Relative cross-section uncertainty [%]	
Source	e+jets	μ+jets
Statistical uncertainty	±43	±29
Object selection		
Lepton reconstruction, identification, trigger	±3	±2
Jet energy reconstruction	±13	±11
b-tagging	-10 / +15	-10 / +14
Background rates		
QCD normalisation	±30	±2
W+jets normalisation	±11	±11
Other backgrounds normalisation	±1	±1
Signal simulation		
Initial/final state radiation	-6 / +13	±8
Parton distribution functions	±2	±2
Parton shower and hadronisation	±1	±3
Next-to-leading-order generator	±4	±6
Integrated luminosity	-11 / +14	-10 / +13
Total systematic uncertainty	-38 / +43	-23 / +27
Statistical + systematic uncertainty	-58 / +61	-37 / +40